Direct Imaging of Exoplanets: Science & Techniques
Proceedings IAU Colloquium No. 200, 2005
C. Aime and F. Vakili, eds.

doi:10.1017/S1743921306009719

The Optical Telescope Assembly for the Terrestrial Planet Finder Coronagraph: Design and Analysis Results

R. G. Ohl[1], A. J. Martino[1], N. F. Martin[1] and the TPFC team

[1]NASA/Goddard Space Flight Center, Greenbelt, MD 20771, USA
email: raymond.g.ohl@nasa.gov

Abstract. The Terrestrial Planet Finder Coronagraph (TPFC) is a National Aeronautics and Space Administration (NASA) exploration mission to directly detect and characterize terrestrial exoplanets at visible and near-infrared wavelengths. The TPFC mission is currently in a "pre-formulation" stage where requirements and designs are traded. TPFC must distinguish a planet that is more than 10 orders of magnitude fainter than its parent star at a separation of 62 mas ($\lambda = 600$ nm). Coronagraphic detection requires a large aperture telescope to resolve the exoplanet from its parent star, and great system (wavefront) stability during detection and characterization. This paper discusses the design considerations, trade studies and analysis leading to the current, "reference" design for the TPFC telescope. We present the salient features of the design and the most significant structural, thermal and optical analysis results. We also discuss the planned model validation and performance verification approach.

Keywords. telescopes, instrumentation: high angular resolution.

1. Introduction

Ford, *et al.* (2005) present an overview of the TPFC mission and baseline design ("flight baseline 1," FB1). The Jet Propulsion Laboratory, California Institute of Technology (JPL) manages the mission. NASA/Goddard Space Flight Center (GSFC) is responsible for the optical telescope assembly (OTA; Figure 1)

The primary mirror (PM) aperture is an 8×3.5 m ellipse. The 62 mas inner working angle drives the 8 m dimension and the perpendicular axis set by the shroud of the baseline launch vehicle (Boeing Delta IV-H). Diffraction produces an elliptical point spread function, so the highest spatial resolution is along the long dimension of the PM.

Shaklan, *et al.* (2005) describe the coronagraph instrument and requirements. The error budget contains static and dynamic terms. The dynamic requirements are driven by the speckle subtraction scheme, in which a stationary planet is separated from a speckle pattern that moves as the telescope is dithered 30° about its axis. The OTA wavefront must thus remain stable to ∼0.1 nm for certain Zernike components during the ∼8 hour integrations associated with dithering. The SM and M3 must remain aligned to the PM to better than of-order 10 nm in translations and 10 nrad in rotations during an integration. Content, *et al.* (2005) list static and dynamic WFE requirements for OTA component figure and alignment tolerances.

For planet finding, the capture range of the coronagraph deformable mirrors (DM) and the dynamic effects of "beam walk" drive the OTA static wavefront error (WFE) requirements for low- and mid-spatial frequency errors. A second instrument, the "general astrophysics instrument" (GAI), observes a wide field of view (∼4×4 arcmin) around the target star. GAI science and higher-order effects on the coronagraph thus drive high

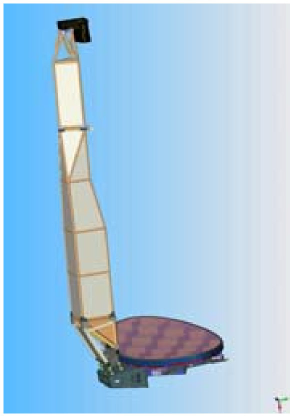

Figure 1. TPFC OTA (Ho/JPL, Engler/GSFC).

Table 1. OTA mirror prescriptions.

Name	Physical size (m)	Off-axis distance (m)	R(m)	$f/\#$	k
PM	8.0×3.5	2.3	26.75	3.82	-1.0019
SM	0.89×0.425	0.237	3.041	4.13	-1.47
M3	0.29×0.31		∞		

spatial frequency WFE tolerances — scattered light from the target star contributes to background on the GAI image plane. For TPFC, bands of WFE spatial frequency are defined relative to the correctable band limit of a high density, "fine" DM placed downstream at a pupil image of the PM. A power spectral density (PSD) specification is generated for each optic using a system performance model based on scalar diffraction theory. The integrated, static surface error requirement for the PM and secondary mirror (SM) is 5.4 nm RMS, while the requirement for the M3 fold mirror is 1.2 nm RMS. Both static and dynamic requirements have implications for mirror fabrication and subsystem- and OTA-level integration and test (I&T). We expect future work to somewhat relax the low-order WFE specification.

The mirrors are coated with protected silver. Wavefront amplitude variations also degrade performance, so reflectance uniformity over the PM must be better than ~0.5 % and is specified as a function of spatial frequency.

Driving mechanical requirements include launch loads, launch vehicle packaging and on-orbit vibration/jitter. Requirements and mitigation schemes are in flux, but we are keeping the minimum first resonant frequency of the payload above ~10 Hz.

The WFE stability requirements lead to challenging thermal stability tolerances, although large static thermal gradients are tolerable. For example, we require temperature stability of-order 1 mK on the PM during a science integration, while static gradients of-order 1 K are permitted.

2. Design and analysis

A schematic of the OTA FB1 concept is shown in Figure 1. The optical path starts at the 8×3.5 m elliptical, off-axis parabolic PM. The SM reflects the light toward a tertiary, flat, fold mirror (M3) that directs the beam into the coronagraph. A pick-off mirror with a through hole at the OTA focus sends the outer portion of the field to the GAI. The

https://doi.org/10.1017/S1743921306009719 Published online by Cambridge University Press

PM is mounted semi-kinematically using a textbook, three-bipod flexure scheme to a metering structure (MS). The MS supports a set of heaters for maintaining the PM at ~293 K. The SM is attached to a deployable tower. A laser "metrology truss" and SM hexapod mechanism actively correct for rigid body motions of the SM relative to the PM during a science integration(Shaklan, *et al.* 2004).

The results of several trade studies are critical to the FB1 design: monolithic vs. segmented PM aperture, Gregorian vs. Ritchey-Chrétien (RC) optical prescription, on-orbit WFE correction method, mirror blank material, "closed- back" vs. "open-back" mirror blank structural design and PM aperture shape (Content, *et al.* 2005).

The Lyot coronagraph design and high contrast requirement drive the architecture to an unobstructed, monolithic aperture. Very tight requirements on segment alignment stability and edge diffraction control rule out a segmented PM approach.

The FB1 OTA prescription is an off-axis RC design (Table 1). Compared to a Gregorian, the RC better accommodates packaging requirements for a given PM speed. The convex SM provides better polarization performance and more forgiving alignment sensitivity than a concave SM. However, it is more difficult to fabricate and test a meter-class, convex SM of this quality. Designs with one and three powered mirrors were also considered, but rejected (Howard, *et al.* 2005).

The OTA requires ~5 μm of on-orbit WFE adjustment to correct for uncertainties in the prediction of PM ground-to-orbit surface error change due to gravity sag and compensating technology and modeling/test uncertainty. The FB1 design incorporates a "coarse DM" early in the coronagraph optical train. This DM has long-stroke actuators capable of correcting microns of low-order WFE, producing an output that is within the capture range of the later, finer pitch, low-stroke DMs. Future work will compare this concept with requirements for OTA manufacture, assembly and I&T. Actuated PM designs are under consideration and address mission requirements to different degrees.

The PM material trade is primarily driven by the thermal stability requirement (Section 1). The structure must be optimized for low-weight and high-stiffness to satisfy requirements from manufacture through launch. Such a lightweight mirror does not conduct heat well, so the thermal stability parameter (i.e., the ratio of conductivity to coefficient of thermal expansion, CTE) is a poor guide in this case. Heat flow is dominated by radiative, not conductive, coupling. This drives the PM to materials engineered for low-CTE and available in large size — i.e., ULE® and Zerodur®. Even for these materials, temperature changes must be limited to the ~1 mK level over an integration. We considered many other factors like blank manufacturing capability, uniformity of CTE and material hardness for polishing, thermal hysteresis and radiation-induced dimensional change. We choose ULE® for the FB1 design, with some reservations.

We considered two structural designs for the PM blank: a "closed-back" or "sandwich" construction and an "open-back," triangular isogrid design (Content, *et al.* 2005). We examined their structural, acoustic and thermal performance. The open-back design is structurally inferior to the closed-back at this high-aspect ratio. Structural analysis showed first resonant frequencies of ~25 Hz for the closed-back and ~14 Hz for the open-back. Acoustic analysis showed higher launch loading for the open-back design. We built a highly detailed thermal model of a single, hexagonal piece of the PM. This analysis showed that the face sheet of an open-back mirror has better radiative communication to heater assemblies mounted around the mirror. Thermal analysis of the observatory using a lower-detail, integrated model showed small temperature changes on the PM during a dither maneuver. While thermal gradients in the open-back model are much smaller, the closed-back model performs with good margin against the <1 mK dynamic gradient requirement. The mechanical advantages drive FB1 to the closed-back design.

https://doi.org/10.1017/S1743921306009719 Published online by Cambridge University Press

To analyze stray light performance, we built non-sequential, bi-directional reflectance distribution function models using the PSD specifications and a simple baffle design. Although invalid for very near angles, we predicted the point source transmission (PST) of the OTA and compared irradiance to the Zodiacal background. We compared the performance of the RC and Gregorian designs. For the Gregorian, a PM focus field stop shades the SM from illumination from the PM by sources outside the field. This makes microroughness less critical for mirrors after that stop. We found that the Gregorian's PST is less than a factor of a few lower than the RC PST for angles $\lesssim 3.5°$. We conclude that the different in irradiance does not alone warrant a change from the RC design.

3. Integration and test

The verification/validation approach is developing in parallel with the design (Smith, *et al.* 2005). Ideally, one would test the OTA under flight-like conditions on the ground to validate requirements and verify performance. However, contrast $<10^{-10}$ and stability $<10^{-11}$ may not be obtainable during testing. Therefore, we are planning a program that maximizes direct test and uses analysis to fill-in where testing is not possible or is prohibitively expensive. Test results feed back to the design early in the project so that we build an OTA that can be verified.

The modeled relationship between contrast and OTA output and component characteristics are the core of this approach (validated by sub-scale and flight hardware testing). Testing will be correlated with models starting at the lowest level of assembly or component test through integration, maintaining "traceability" from one step to the next.

Acknowledgements

We gratefully acknowledge the contributions of the JPL, GSFC and industry teams working on mission pre-formulation. Reference herein to any specific commercial product, process or service does not constitute or imply its endorsement by NASA or JPL.

References

Content, D., Ohl, R., Cafferty, T., Cohen, E., Egerman, R., Engler, C., Fantano, L., Feher, P., Green, J., Ho, T., Howard, J., Hunyadi, S., Irish, S., Jackson, C., Kissil, A., Kwack, E., Martin, N., Martino, A., Pattison, J., Peabody, S., Smith, A., & Weng, I. 2005, in: M. Kahan (ed.), *Optical Modeling and Performance Predictions II*, Proceedings of SPIE 5867, in press

Ford, V., Levine-West, M., Kissil, A., Kwack, E., Ho, T., Dumont, P., Lisman, D., Feher, P., & Cafferty, T. 2005, in: C. Aime & F. Vakili (eds.), *Direct Imaging of Exoplanets: Science and Techniques IAU Colloquium*, IAU Colloquium No. 200 (Cambridge University Press), this volume

Howard, J., Mouroulis, P., Thompson, A., Smith, A., Content, D., Ho, T., Jackson, C., Ohl, R., & Shaklan, S. 2005, in: P. Mouroulis, W. Smith & R. Johnson (eds.), *Current Developments in Lens Design and Optical Engineering VI*, Proceedings of SPIE 5874, in press

Shaklan, S., Marchen, L., Zhao, F., Peters, R., Ho, T., & Holmes, B. 2004, in: L. Peterson & R. Guyer (eds.), *Space Systems Engineering and Optical Alignment Mechanisms*, Proceedings of SPIE 5528, 22

Shaklan, S., Balasubramanian, K., Green, J., Hoppe, D., Lay, O., Lisman, D., & Mouroulis, P. 2005, in: C. Aime & F. Vakili (eds.), *Direct Imaging of Exoplanets: Science and Techniques IAU Colloquium*, IAU Colloquium No. 200 (Cambridge University Press), this volume

Smith, A., Blaurock, C., Krim, M., Levine, M., Liu, A., Martino, A., Ohl, R., & Pitman, J. 2005, in: D. Coulter (ed.), *Techniques and Instrumentation for Detection of Exoplanets II*, Proceedings of SPIE 5905, in press